IRANIAN JOURNAL OF CATALYSIS

Pistachio peel biomass derived magnetic nanoparticles Fe_3O_4@C-SO_3H: a highly efficient catalyst for the synthesis of isoxazole-5(4*H*)-one, 1-amido alkyl-2-naphthol, pyrano[2,3-c]pyrazole and 2,3-dihydro quinazoline-4(1*H*)-one derivatives

Fatemeh Ghorbani[a*] and Seied Ali Pourmousavi [a,b]

a) School of Chemistry, Damghan University Damghan, Iran
b) Institute of Biological Science, Damghan University Damghan, Iran

Received 4 July 2021; received in revised form 12 February 2022; accepted 10 March 2022 (DOI: 10.30495/IJC.2022.690999)

ABSTRACT

Green chemistry has fostered research on recyclable, insoluble, and easily separable heterogeneous catalysts. Carbon materials are widely used for renewable energy and environmental studies. Here, we used green Pistachio peel, a biomass waste for the synthesis of magnetic carbon-based solid acid (Fe_3O_4@C-SO_3H) by carbonization and sulfonation. The physicochemical properties of the nanocatalyst were characterized using XRD, FT-IR, FE-SEM, TGA, VSM, and TEM. The catalytic activity of Fe_3O_4@C-SO_3H was investigated in the synthesis of isoxazole-5(4*H*)-one, 1-amido alkyl-2-naphthol, pyrano[2,3-c]pyrazole, and 2,3-dihydro quinazoline-4(1*H*)-one derivative, and some of the synthesized compounds were screened for their anti-microbial activity. Furthermore, the recovery and reuse of the catalyst were demonstrated six times without detectible loss inactivity. The concentration of H^+ loaded on the Fe_3O_4@C-SO_3H was reported to be 1.3 mmol g^{-1}. The well-defined Fe_3O_4@C-SO_3H core–shell heterostructures exhibited high stability, efficient recyclability (6 cycles).

***Keywords**: Magnetic nanocatalyst, biomass, pistachio peel, isoxazole, amido alkylnaphthol, pyrano pyrazole, dihydro quinazolin.*

1. Introduction

Multicomponent reactions (MCRs) are effective methods for the practical construction of a wide range of heterocyclic compounds in a single process with structural diversity and complexity from simple and inexpensive starting materials via the generation of several bonds in a single synthetic operation [1-7].
The isoxazole-5(4H)-one, also called isoxazoline, ring systems represent important molecular structures, which have been employed as the precursors in the synthesis of interesting organic molecules [8]. They have been known to show antibacterial [9], antifungal [10], tyrosinase inhibitory [11], anticancer [12], anti-obesity [13], anti-androgen [14], CDP-ME kinase inhibitor [15], anti HIV [16], fungicide [17], and insecticides [18] activities. Also, the isoxazole-5-(4H)-one motif as the powerful electron acceptor is likely to be a good candidate for organic nonlinear optical (NLO) materials [19], photonic applications [20], and solar cells [21]. One of the most attractive methods of obtaining isoxazole-5(4H)-ones is the cyclo condensation of hydroxylamine hydrochloride with β-ketoesters and various aldehydes in the presence of various types of catalysts, including sodium acetate and tungsten lamp [21], potassium phthalimide (PPI) [22], potassium hydrogen phthalate (KHP) [23], tetrabutylammonium perchlorate (TBAP)/glycine/sodium oxalate [24] and silica (SiO_2–H_2SO_4) [25].

The 1-amido alkyl-2-naphthol derivatives are important organic compounds found in anti-inflammatory, anthelmintic, antibacterial, and antiviral agents [26]. Some 1-amido alkyl-2-naphthols are well-known intermediates to synthesize 1-amino alkyl-2-naphthols (Betti bases) as pharmaceutically active molecules with depressor, hypertensive, and bradycardia [27]. Furthermore, derivatives of 1-amido alkyl-2-naphthol

*Corresponding author:
E-mail address: *fatemehghorbani216@yahoo.com* (**F. Ghorbani**)

act as precursors for the synthesis of interesting molecules with biological activity, including antibiotic [28], antihypertensive [29], analgesic [30], antimalarial [31], antitumor [32], antirheumatic [33], antianginal [34], and anticonvulsant [35]. Owing to the importance of such biologically active scaffolds and their occurrence in natural products, their synthesis is interesting to researchers. A one-pot MCR of β-naphthols, aldehydes, and amides is an excellent practical synthetic technique for the synthesis of 1-amido alkyl-2-naphthols, which is catalyzed by several catalysts such as sulfanilic acid [36], cellulose-SO3H [37], zirconocene dichloride (Cp_2ZrCl_2) [38], copper p-toluenesulfonate (CPTS) [39], tin tetrachloride ($SnCl_4.5H_2O$) [40] and magnetic nanoparticles supported (iminoethyl)phenyl)imino)methyl)phenol Cu (II) or Zn (II) Schiff base complexes [41].

Pyrano pyrazoles are an important category of heterocyclic compounds, which play a significant role in the pharmaceutical field and biologically active compounds. Compounds bearing the pyrano pyrazole system have been found to have various biological activities, for instance, antimicrobial [42], analgesic [43], vasodilator [44], anticancer [45], anti-inflammatory [46], molluscicidal [47], anti fungicidal [48], and also as biodegradable agrochemicals [49], furthermore, some of these compounds are commonly employed in industries such as cosmetics and pigments [50]. Various catalysts and conditions have been used to synthesize pyrano pyrazoles through a four-component reaction of aldehydes, ethyl acetoacetate, malononitrile with hydrazine hydrate. Some of those catalysts are triethylamine [51], p-dodecylbenesulfonic acid (DBSA) [52], hexadecyltrimethylammonium bromide (HTMAB) [53], ammonium acetate [54] and silicotungstic acid ($H_4[SiW_{12}O_{40}]$) [55].

The heterocyclic fused rings quinazolines have attracted a huge consideration because of their expanded applications in the field of pharmaceutical chemistry [56]. Many substituted quinazoline derivatives possess a wide range of bioactivities such as antimalarial [57], anticancer [58], antimicrobial [59], antifungal [60], antiviral [61], antihypertensive [62], anti-inflammatory [63], anti-diabetes [64], muscle relaxant [65], antitubercular [66], antiobesity [67], anticonvulsant [68] and many other ones. Quinazolines compounds are used in the preparation of various functional materials for synthetic chemistry and are also present in molecules of various drugs. Several synthetic routes have been widely used for the preparation of quinazoline derivatives. These compounds have been synthesized in the presence of a variety of homogeneous or heterogeneous catalysts such as molecular iodine (I2) [69], cyanuric chloride [70], morpholinoethanesulfonic acid [71], silica-supported polyphosphoric acid (SiO_2-PPA) [72], NH_4Cl [73] or by electrochemical reactions.

Solid acid catalyst has been applied in organic transformations due to their high catalytic activity, operational simplicity, cost-effectiveness, and recyclability [74-79]. Functionalized magnetic nanoparticles, on the other hand, have become a valuable and efficient catalyst in green organic transformations because they provide a convenient way of using a magnet for the isolation of stimuli and in chemical reactions facilitates the recovery of expensive catalysts from the reaction mixture, due to easy separation by a magnet avoiding the need for the tedious workup procedure [80-84].

In this work, we have developed a low-cost approach for synthesizing a magnetic carbon-based solid acid catalyst (Fe_3O_4@C-SO_3H) by using green Pistachio peel biomass waste as a carbon source. The as-prepared nanocatalyst was characterized by XRD, FT-IR, FE-SEM, TGA, VSM, and TEM. The catalytic performance of the as-prepared catalysts was examined in the synthesis of isoxazole-5(4H)-one, 1-amido alkyl-2-naphthol, pyrano[2,3-c]pyrazole, and 2,3-dihydro quinazolin-4(1H)-one derivative, and some of the synthesized compounds were screened for their anti-microbial activity.

2.Experimental

2.1 General

All chemicals were purchased from commercial sources and were used without further purification. The products were characterized by comparison of their physical data with those of known samples or by their spectral data. Melting points were measured on a Buchi 510 melting point apparatus and are uncorrected. Nuclear magnetic resonance (NMR) spectra were recorded at ambient temperature on a BRUKER AVANCE DRX-400 MHz using $CDCl_3$ or DMSO-d_6 as the solvent. Fourier-transform infrared spectroscopy (FT-IR) spectra were recorded on a Perkin-Elmer RXI spectrometer. Thermogravimetric analysis (TGA) was conducted from room temperature to 750 ºC under argon atmosphere using a BAHR-Thermoanalyse simultaneous thermal analyzer STA 503 instrument with aluminium oxide reference. X-ray diffraction (XRD) patterns of samples were taken on a Philips X-ray diffract meter Model PW 1840. The particle morphology was examined by Field emission scanning electron micro1scopy (FE-SEM) (Philips XL30 scanning electron microscope). Transmission electron microscopy (TEM) observations were performed using a Zeiss TEM- LEO 910 apparatus operating at 100 kV.

The development of reactions was monitored by thin layer chromatography (TLC) analysis on Merck pre-coated silica gel 60 F_{254} aluminum sheets, visualized by ultraviolet (UV) light.

2.2. Catalyst preparation

2.2.1. Synthesis of Fe_3O_4 nanoparticles

The magnetic core was synthesized by the coprecipitation method [85]. The $FeCl_3.6H_2O$ and $FeCl_2.4H_2O$ with the molar ratio of 2:1 were dissolved in water. Then, NH_3 solution was added to keep the pH between 11 and 12. The magnetic core was obtained by magnetic attraction and washed with water. The products were then dried at 60 °C in vacuum for 6 h for further characterization.

2.2.2. Synthesis of Fe_3O_4 @C-SO_3H

Green Pistachio peel was obtained from Damghan's Pistachio gardens. The green Pistachio peel was washed with water and was oven-dried at 70 ˚C for 6 h then was ground to powder by an electric spice grinder. Green Pistachio peel powder (10.0 g) and water (80 mL) were mixed and stirred at room temperature [86]. Then, 2 g of magnetic core Fe_3O_4 nanoparticles was added, the resulted mixture was dispersed using ultrasonic vibration. The mixture was transferred to the 100 mL Teflon-lined stainless steel autoclaves and heated in an oven at 180 ˚C for 12 h. The carbon intermediate was magnetically attracted, washed with water and ethanol, and dried at 60 °C in an oven under vacuum for 12 h. The resulted compound is denoted as Fe_3O_4 @C.

Then a mixture of Fe_3O_4 @C (1.0 g) and concentrated sulfuric acid (>98%, 10 mL) was mixed and stirred at room temperature. After being stirred for 1 h, the resultant mixture was transferred into a 100 mL sealed Teflon-lined autoclave and kept at 180 °C for 12 h. After cooling to room temperature, the resulting black solid was washed with hot deionized water and ethanol several times until sulfate ions were no longer detected, then dried at 60 °C in an oven under vacuum for 12 h. The as-prepared catalyst is denoted as Fe_3O_4 @C-SO_3H.

2.2.3. Solid acid titration

The acid loading of (Fe_3O_4@C-SO_3H) MNPs (total acidity) was determined by acid-base titration. The acid-based titration was achieved by treating 40 mg of Fe_3O_4@C-SO_3H MNPs with 50 ml of a (0.01 M) NaOH solution at room temperature for 2 h. The catalysts were separated by filtration. The resulted solution was titrated to neutrality using a (0.01 M) HCl solution and phenolphthalein solution as the indicator to determine the total acidity of Fe_3O_4@C-SO_3H MNPs, Including sulfonic acid, carboxylic acid and phenolic groups (**Scheme 1**) [86].

The sulfonic acid loading groups of the functionalized Fe_3O_4@C-SO_3H MNPs were determined by titration using NaCl solution. A mixture of 40.0 mg of the sample with 10 ml of a saturated NaCl solution was stirred at room temperature for 24 h. The catalyst was separated by filtration. The resulted solution was titrated to neutrality using a (0.01 M) NaOH solution and phenolphthalein as the indicator [86].

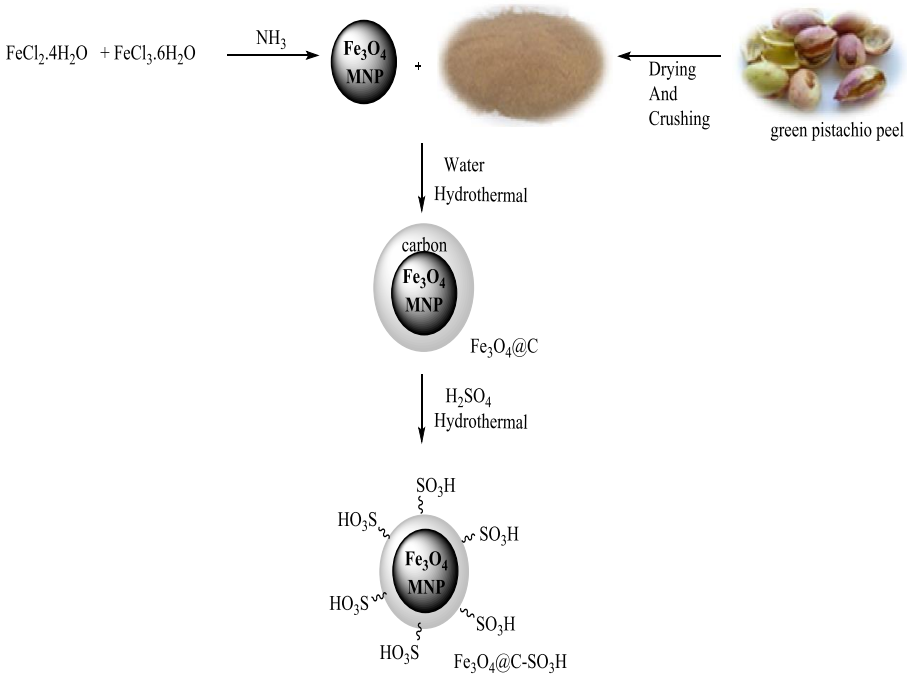

Scheme 1. The synthetic route of the magnetic carbon-based solid acid

2.3. Catalytic performance

*2.3.1. General procedure for the synthesis of α,β-unsaturated isoxazole-5(4H)-ones **(4a–l)***

A mixture of hydroxylamine hydrochloride (0.0695 g, 1.0 mmol), β-ketoester (1.0 mmol), and Fe_3O_4@C-SO_3H MNPs (0.03 g) in 5 mL of distilled water was stirred at room temperature (rt) for 10 min; then, aryl/heteroaryl aldehyde (1.0 mmol) was added to the vessel reaction. The reaction mixture was stirred at room temperature until the reaction was completed (monitored by TLC analysis). After the completion of the reaction, the catalyst was separated by an external magnet and the precipitate was separated by simple filtration and the products were crystallized from ethanol (95%) to afford the title pure compounds.

*3-Methyl-4-(4-methylbenzylidene)isoxazole-5(4H)-one **(4b)***

^{1}H-NMR (400 MHz, $CDC1_3$): d 2.33 (s, 3H), 2.48 (s, 3H), 7.36 (d, *J* = 8.1 Hz, 2H), 7.42 (s, 1H), 8.32 (d, *J* = 8.4 Hz, 2H); ^{13}C NMR (100 MHz, $CDC1_3$): d 11.6, 22.1, 118.2, 129.8, 129.9, 134.2, 145.8, 150.2, 161.4, 168.3.

*4-(4-(Dimethylamino)benzylidene)-3-methylisoxazole5(4H)-one **(4d)***

H NMR (400 MHz, $CDC1_3$): d 2.27 (s, 3H), 3.19 (s, 6H), 6.75 (dd, *J* = 1.2, 8.4 Hz, 2H), 7.24 (s, 1H), 8.43 (d, *J* = 8.4 Hz, 2H); ^{13}C NMR (100 MHz, $CDC1_3$): d 11.7, 40.1, 110.9, 111.5, 121.5, 137.7, 149.3, 154.2, 161.7, 170.2.

*3-Methyl-4-(thiophen-2-ylmethylene)isoxazole-5(4H)one **(4h)***

H NMR (400 MHz, $CDC1_3$): d 2.32 (s, 3H), 7.29 (t, *J* = 4.8 Hz, 1H), 7.64 (s, 1H), 7.95 (d, *J* = 4.8 Hz, 1H), 8.13 (d, *J* = 3.6 Hz, 1H); ^{13}C NMR (100 MHz, $CDC1_3$): d 11.5, 114.6, 128.9, 136.5, 139.2, 139.6, 141.5, 160. 7, 168.7.

*2.3.2. General procedure for the synthesis of 1-amido alkyl-2-naphthols **(7a-l)***

A mixture of substituted benzaldehyde (1.0 mmol), 2-naphthol (1.0 mmol), amide (1.0 mmol) and Fe_3O_4@C-SO_3H MNPs (0.04 g) was stirred at 70 °C in an oil bath. After completion of the reaction (using TLC analysis), the hot ethanol was added to the resulting mixture and the catalyst was separated by an external magnet and the reaction mixture was allowed to cool to room temperature and solid product was formed.

*N-((2-Hydroxynaphthalen-1-yl)(3-nitrophenyl)methyl)acetamide **(7a)***

^{1}H NMR (400 MHz, DMSO-d_6): δ = 10.14 (s, 1H), 8.62 (d, *J* = 8.0 Hz, 1H), 8.02-7.99 (m, 2H), 7.84 (br, 1H), 7.78 (t, *J* = 8.6 Hz, 2H), 7.59-7.51 (m, 2H), 7.40 (t, *J* = 7.6 Hz, 1H), 7.26 (t, *J* = 7.4 Hz, 1H), 7.18 (d,*J* = 8.7 Hz, 1H), 7.16 (t, *J* = 8.0 Hz, 1H), 2.02 (s, 3H); ^{13}C NMR (100 MHz, DMSO-d_6): δ = 170.3, 153.9, 148.2, 145.9, 133.4, 132.7, 130.5, 130.1, 129.2, 128.9, 127.3, 123.2, 123.1, 121.8, 120.9, 118.9, 118.3, 48.2, 23.1.

*N-((2-Hydroxynaphthalen-1-yl)(4-nitrophenyl)methyl)acetamide **(7b)***

^{1}H NMR (400 MHz, DMSO-d_6): δ = 10.07 (s, 1H), 8.53 (d, *J* = 7.9 Hz, 1H), 8.10 (d, *J* = 8.8, 2H), 7.74-7.82 (m, 3H), 7.44-7.33 (m, 3H), 7.25 (t, *J* = 7.5 Hz, 1H), 7.19 (d, *J* = 8.8 Hz, 1H), 7.14 (d, *J* = 7.9 Hz, 1H), 1.98 (s, 3H).

*1-((2-Hydroxynaphthalen-1-yl)(phenyl)methyl)urea **(7c)***

^{1}H NMR (400 MHz, DMSO-d_6): δ = 9.97 (s, 1H), 7.75-7.83 (m, 3H), 7.82 (d, *J* = 7.9 Hz, 1H), 7.41-7.12 (m, 7H), 6.94 (s, 1H), 5.86 (s, 2H).

*2.3.3. General procedure for the synthesis of pyrano[2,3-c]pyrazole derivatives **(10a-l)** .*

A mixture of aryl aldehyde (1.0 mmol), phenylhydrazine/hydrazine hydrate (1.0 mmol), ethyl acetoacetate (1.0 mmol), malononitrile (1.0 mmol) and Fe_3O_4@C-SO_3H MNPs (0.03 g) was stirred in water (5 mL) at room temperature. After completion of the reaction (monitored by TLC), the catalyst was separated by an external magnet and the product was filtered off, washed with small amounts of water (5 mL) and then recrystallized from hot ethanol to give the pure products.

*6-amino-3-methyl-4-(p-tolyl)-1,3a,4,7a-tetrahydropyrano[2,3-c]pyrazole-5-carbonitrile **(10b)***

^{1}H NMR (400 MHz, DMSO-d_6) δ ppm 1.77 (s, 3H, CH_3), 4.79 (s, 1H, CH), 6.98 (s, br, 2H, NH_2), 7.46 (d, 2H, *J* = 8.4 Hz, ArH), 8.20 (d, 2H, *J* = 8.6 Hz, ArH), 12.13 (s, 1H, NH); ^{13}C NMR (100 MHz, DMSO-d_6) δ ppm 10.1, 35.1, 61.0, 98.6, 120.5, 123.9, 129.1, 135.9, 146.5, 149.2, 150.7, 161.2.

*2.3.4. General procedure for the synthesis of 2,3-dihydro quinazolin-4(1H)-ones **(12a-l)***

To a solution of 2-aminobezamide (1.0 mmol) and substituted benzaldehyde (1.0 mmol) in water (5 mL), Fe_3O_4@C-SO_3H MNPs (0.03 g) was added. The mixture

was stirred at room temperature. After completion of the reaction, as indicated by TLC (ethyl acetate: n-hexane 1:1), the catalyst was separated by an external magnet and the precipitate was filtered off. Finally, the crude product was purified by recrystallization from EtOH to afford the corresponding 2,3-dihydroquinazolin-4-(1*H*)-ones.

2,3-dihydro-2- phenylquinazolin-4(1H)-one ***(12a)***

^{1}H NMR (400 MHz, DMSO): δ 5.75 (s, 1H), 6.67 (t, 1H), 6.76 (d, *J*= 8 Hz, 1H), 7.11 (s, 1H), 7.24 (t, 1H), 7.34-7.39 (m, 3H), 7.49 (d, *J*= 8 Hz, 2H), 7.61 (d, *J*= 6.4 Hz), 8.29 (s, 1H, br).

2,3-dihydro-2-(3,4- dimethoxy phenyl) quinazolin-4(1H)-one ***(12h)***

^{1}H NMR (400 MHz, DMSO): δ 3.74 (s, 3H), 3.75 (s, 3H), 5.69 (s, 1H), 6.67 (t, 1H), 6.75 (dd, *J*= 8 Hz, 1H), 6.93-6.98 (m, 2H), 7.01 (s, 1H, br), 7.24 (m, 1H), 7.60 (dd, *J*= 8 Hz), 8.16 (s, 1H).

2,3-dihydro-2-(3,4,5-trimethoxy phenyl) quinazolin-4(1H)-one ***(12i)***

^{1}H NMR (400 MHz, DMSO): δ 3.64 (s, 3H), 6.67-6.71 (m, *J*= 8 Hz, 1H), 6.76 (dd, *J*= 8 Hz, 1H), 6.84 (s, 2H), 7.04 (s, 1H, br), 7.26 (m, *J*= 8 Hz, 1H), 7.62 (s, *J*= 7.8 Hz ,1H), 8.21 (s, 1H). ^{13}C NMR (400 MHz, DMSO): 56.34, 60.34, 67.34, 104.86, 104.86, 114.89, 115.48, 117, 127.82, 133.75, 137.03, 137.03, 137.03, 137.97, 148.50, 153.18, 164.16.

Anti-microbial testing

Some of the prepared compounds 1-4 were screened for their antimicrobial activity. The preliminary activity was determined by the disc diffusion method. In this work, Escherichia coli and Staphylococcus aureus bacterial strains were used. The compounds were dissolved in DMSO at a concentration of 1 mgmL^{-1} [25, 41].

3. Results and Discussion

3.1. Characterization of the novel magnetic carbon-based solid acid

3.1.1. Acidity test of Fe_3O_4@C-SO_3H MNPs

Green pistachio peel biomass waste was used as a carbon source for the synthesis of the novel magnetic carbon-based solid acid by a hydrothermal method. To increase the acidity of the catalyst, the sulfonation was done by concentrating sulfuric acid at 180 °C in a sealed Teflon-lined autoclave. In this process, polycyclic aromatic carbon sheets in Fe_3O_4@C MNPs were sulfonated.

The amount of introduced sulfonic acid (-SO_3H) groups was 1.3 mmol H^+ g^{-1}, quantified by an ion exchange of H^+ ions of the sulfonic acid with NaCl, followed by titration of the resulting filtrate with NaOH. On the other hand, the number of H^+ determined by acid–base titration was 2.8 mmol H^+ g^{-1} for total acidity including –SO_3H, -COOH, and phenolic -OH groups based on reaction with NaOH and then back-titration by HCl solution.

The acidity of the magnetic carbon-based solid acid was derived mainly from the sulfonic acid groups [86], To enhance the acidity of catalyst, the amounts of sulfuric acid were increased. The acidity of 1.3 mmol H^+/g was obtained by the reaction of sulfuric acid (10 ml) and Fe_3O_4@C (1 g). The higher acidity of 2.0 mmol H^+/g was obtained using sulfuric acid (15 ml). However, the magnetic property of this solid acid was decreased because of the corrosion of the magnetic core by sulfuric acid. So, As shown in **Table 1**, the optimized acidity of the catalyst was obtained by the reaction of H_2SO_4 (10 ml) and Fe_3O_4@C (1 g) under hydrothermal conditions.

3.1.2. analysis of Fe_3O_4@C-SO_3H MNPs

The nanocatalyst Fe_3O_4@C-SO_3H was characterized by various microscopic, and spectroscopic techniques such as X-ray diffraction (XRD), Scanning electron microscope (SEM), Transmission electron microscopy (TEM), Fourier-transform infrared spectra (FT-IR), Thermogravimetric (TGA), and Vibrating sample magnetometer (VSM).

The XRD pattern (**Fig. 1. b**) of the magnetic carbon-based solid acid showed the diffraction peaks at 30.4, 35.8 43.2, 51.3, 57.4 and 62.9, which were attributed to the (220), (311), (400), (422), (511), and (440) planes of Fe_3O_4, respectively. The result indicated that the magnetic iron oxide structure was well kept in the solid acid, which further confirmed the sulfonation process did minor harm to the magnetic cores. For the amorphous carbonaceous shell, the XRD pattern showed many glitches in the baseline, and the broad weak diffraction peak near nine further confirmed the amorphous carbon shell [87].

FT-IR patterns of Fe_3O_4@C-SO_3H MNPs in the wavelength of 400-4000 cm^{-1} are shown in **Fig 1. c**). The carbonization process successfully endows, as demonstrated by the FT-IR spectrum of the catalyst. The broad solid absorbability in 950–1250 cm^1 was attributed to the C–O stretching vibration, which confirmed the high oxygen-containing groups in carbon intermediate. The strong peak in 1058 cm^{-1} confirmed

Table 1. The acidity of catalyst in the reaction of Fe_3O_4@C (1 g) and various amounts of sulfuric acid.

Entry	sulfuric acid (ml)	Acidity (mmol H^+/g)
1	5	0.6
2	10	1.3
3	15	2.0

the S-O, which indicated the sulfonic acid groups were successfully introduced to the carbon shell. The $-SO_3H$ groups give rise to the sharp peaks at 1350 and 1160 cm^{-1} due to asymmetric and symmetric stretching vibrations of $-SO_2-$ groups. As shown in the FT-IR pattern of the catalyst, the broadband around 3600 to 2800 cm^{-1} indicates the presence of −OH in COOH carboxylic and phenolic OH groups. Also, the existing band at 1600 cm^{-1} to 1700 cm^{-1} is due to C=O of COOH and C=C of the poly-aromatic rings of hydrocarbon in the base. This indicates that functional groups including SO_3H, COOH, and OH of phenolic groups were present on the catalyst after sulfonation; the absorption peaks at around 560 cm^{-1} and 580 cm^{-1} could be assigned to the Fe-O absorption in the hematite [88].

The stability of the Fe_3O_4@C-SO_3H catalyst was determined by thermo-gravimetric analysis. The thermal gravimetric (TG) analysis of Fe_3O_4@C-SO_3H was performed over the range of 25 to 800 °C, with a temperature increase rate of 10 °C min^{-1} in a nitrogen atmosphere (**Fig. 1. e**). According to the TG curve, the weight loss processes of Fe_3O_4@C-SO_3H could be divided into two stages. The first weight loss in the field was in the range of 100-150 °C. The second weight loss in the range of 250-300 °C was attributed to the decomposition of the organic layer. Therefore, Fe_3O_4@C-SO_3H is stable below 200 °C, which is enough for constant weight during the catalysis procedure of our experiments [89].

The size of particles was evaluated by FE-SEM, and TEM images of the Fe_3O_4@C-SO_3H catalyst (**Figs. 1a** and **1f**. Both the TEM and SEM showed that the nanoparticles of the Fe_3O_4@C-SO_3H were present and the size of nanoparticles was less than 100 nm and their morphology is spherical. TEM images clearly showed that as-prepared particle has a core–shell structure [90].

The hysteresis loop of Fe_3O_4@C-SO_3H is shown in (**Fig. 1. d**). As can be seen, compared with the high saturation magnetization (57.32 emu/g) of Fe_3O_4, the saturation magnetization (50.77 emu/g) of magnetic Fe_3O_4@C-SO_3H was significantly reduced, because of the thick layer of carbon [91].

3.2.Catalytic studies

3.2.1.Synthesis of α,β-unsaturated isoxazole-5(4H)-ones ***(4a–l)***

Because of our ongoing program for developing greener and sustainable processes for the synthesis of heterocyclic compounds [92-99] here, the catalytic application of Fe_3O_4@C-SO_3H MNPs was examined in the synthesis of α, β-unsaturated isoxazole-5(4H)-ones. The synthesis of *α,β*-unsaturated isoxazole-5(4*H*)-ones was achieved using the multicomponent reaction of various benzaldehyde, hydroxylamine hydrochloride, and *β*-ketoesters in aqueous media at room temperature. To find the best conditions, the reaction between benzaldehyde, hydroxylamine hydrochloride and ethyl acetoacetate was chosen as a model reaction, The influences of various parameters such as reaction temperature, solvent, amount of catalyst were examined to obtain the best possible combination (**Table 2**). Initially, a series of solvents, including H_2O, EtOH, CH_3CN, *n*-Hexane and under solvent-free conditions were studied in the presence of 0.03 g of prepared catalyst. The best result was obtained in aqueous media. Next, the effects of catalyst loading under the aqueous condition and temperature on the model reaction were examined. The results were summarized in **Table 1**. The best results were gained with 0.03 g catalyst in aqueous media at room temperature. The increased temperature and the addition of more catalyst amounts did not lead to better results (reaction time and yield). The important thing is that without the use of catalysts, the reaction did not proceed.

After successfully optimizing the reaction conditions, the cyclo condensation reaction of a range of different aryl/heteroaryl aldehydes was explored, and the results are given in **Table 3**. On the other hand, the reaction of buthyraldehyde, hydroxylamine hydrochloride and ethylacetoacetate did not lead to α,β-unsaturated isoxazole, so aliphatic aldehyde does not react in these conditions.

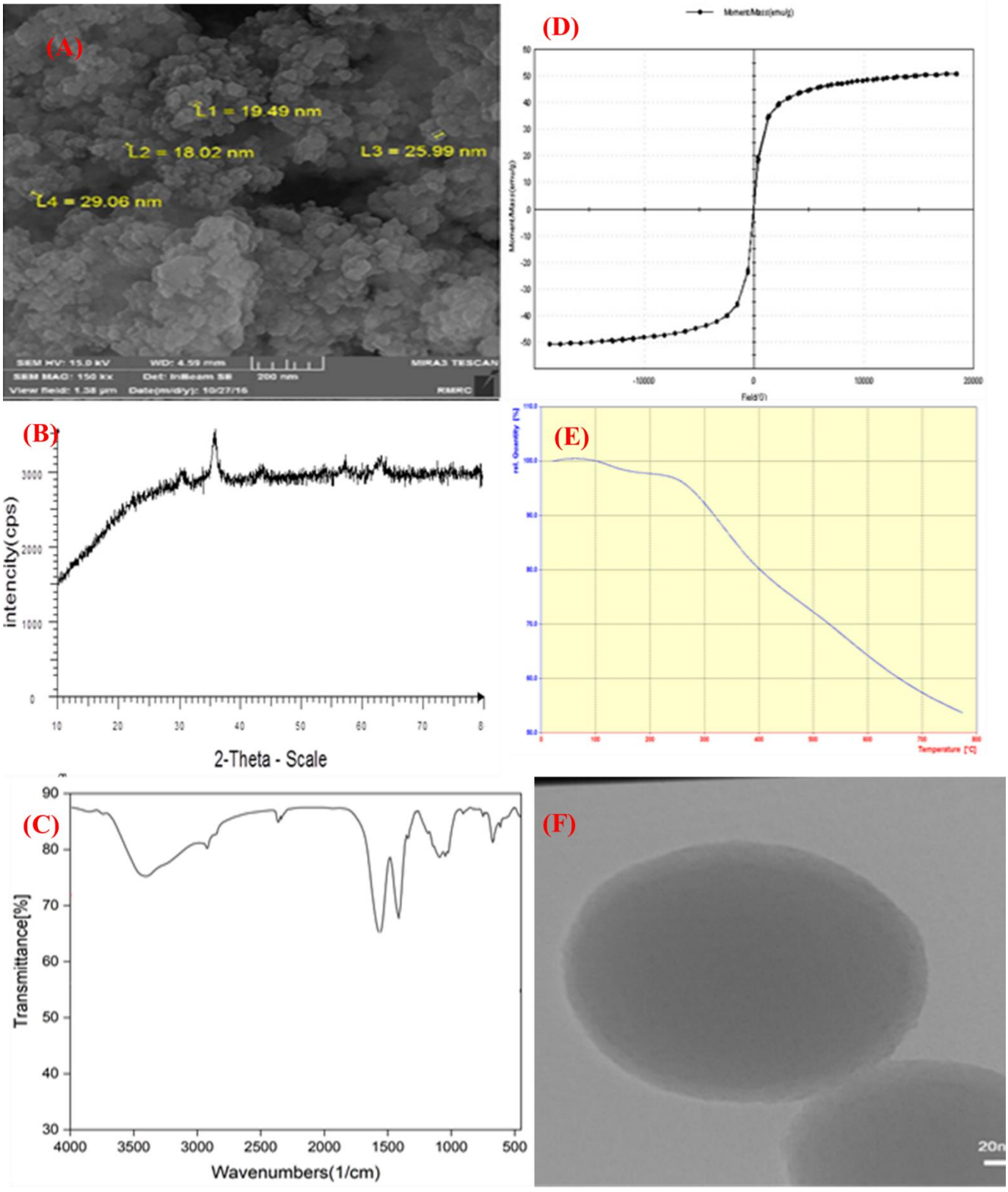

Fig. 1. Analysis and spectra of Fe_3O_4@C-SO_3H MNPs. (A): Scanning Electron Microscopy (SEM), (B): X-ray Diffraction (XRD), (C): Fourier-transform infrared spectra (FT-IR), (D): Vibrating sample magnetometer (VSM), (E): Thermogravimetric analysis (TGA), (F): Transmission electron microscopy (TEM).

Table 2. Screening of the reaction conditions of the model reaction of benzaldehyde, hydroxylamine hydrochloride, and ethyl acetoacetate for the synthesis of 4a in the presence of Fe_3O_4@C-SO_3H MNPs. [a]

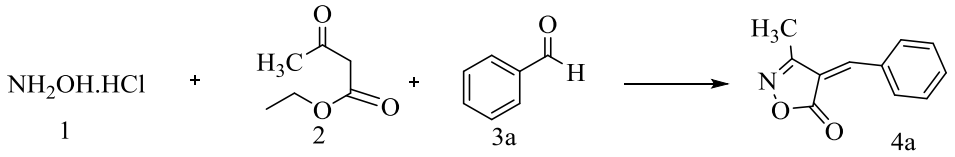

Entry	Catalyst (g)	mmol H^+	T (˚C)	Solvent (5 mL)	Time (min)	Yield (%)
1	0.02	0.026	25	H_2O	10	50
2	0.03	0.039	25	H_2O	10	98
3	0.04	0.052	25	H_2O	10	90
4	-	0	25	H_2O	60	-
5	0.03	0.039	Reflux	H_2O	3	50
6	0.03	0.039	25	EtOH	30	65
7	0.03	0.039	25	n-Hexane	120	0
8	0.03	0.039	25	Solvent-free	30	30
9	0.03	0.039	25	CH_3CN	120	5

[a] The reaction conditions benzaldehyde (1.0 mmol), hydroxylamine hydrochloride (1.0 mmol), and ethyl acetoacetate (1.0 mmol) in the presence of Fe_3O_4@C-SO_3H MNPs under various conditions.

Table 3. Scope of aldehydes and *β*-ketoesters studied for the synthesis of *α, β*-unsaturated isoxazole-5(4*H*)ones (4a–l) catalyzed by Fe_3O_4@C-SO_3H MNPs. [a, b]

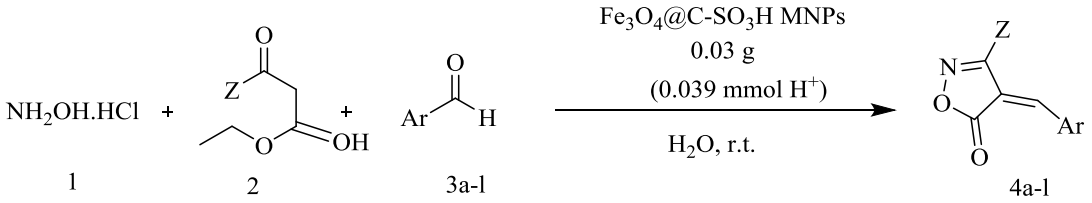

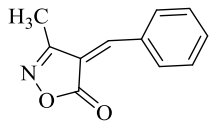	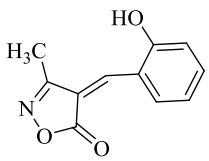	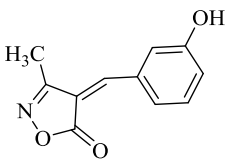	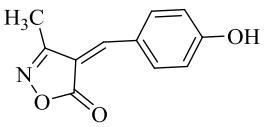
4a; 98%	4b; 96%	4c; 95%	4d; 98%
10 min	20 min	15 min	15 min
141-143 ˚C	198-200 ˚C	202-204 ˚C	125-127 ˚C
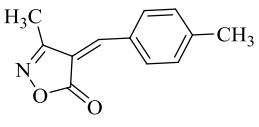	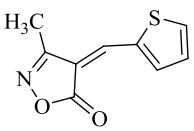	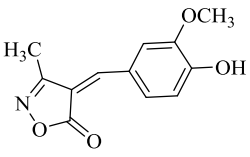	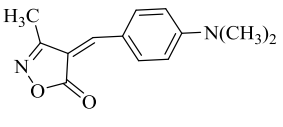
4e; 94%	4f; 90%	4g; 97%	4h; 100%
17 min	25 min	10 min	7 min
135-137 ˚C	146-148 ˚C	211-213 ˚C	226-228 ˚C

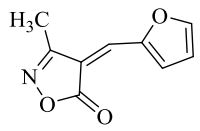	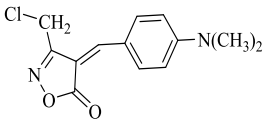	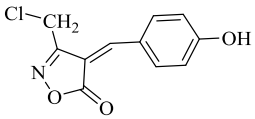	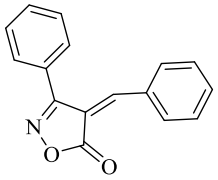
4k; 90%	4j; 96%	4k; 94%	4l; 91%
20 min	12 min	10 min	30 min
239-241 ˚C	179-181 ˚C	182-184 ˚C	214-216 ˚C

[a] The reaction conditions aldehyde (1.0 mmol), hydroxylamine hydrochloride (1.0 mmol), and β-ketoester (1.0 mmol) in the presence of Fe_3O_4@C-SO_3H MNPs (0.03 g) and H_2O (5 mL) at rt. [b]Melting points are listed in Refs: [15-19].

*3.2.2.Synthesis of 1-amido alkyl-2-naphthols **(7a–l)***

The catalytic performances were also investigated in the synthesis of amido alkyl naphthols as multicomponent reactions. For this purpose, a series of trial reactions were performed with a combination of benzaldehyde, 2-naphthol, acetamide to obtain reaction conditions (**Table 4**). Several solvents were screened before concluding that responses were carried out without any solvent and the important thing is that without the use of catalysts, the response did not proceed. Thus, the optimum conditions for the synthesis of 1-amido alkyl-2-naphthols were achieved by treatment of aromatic aldehyde (1 mmol), 2-naphthol (1 mmol), acetamide (1 mmol) in the presence of Fe_3O_4@C-SO_3H MNPs (0.04 g) at 70 ˚C under Solvent-free conditions.

Therefore, we employed the above conditions for the conversion of various aldehydes to the 1-amido alkyl-2-naphthols, the reaction time and the percentage yield of the products are shown in **Table 5**. The reaction of buthyraldehyde, hydroxylamine hydrochloride and ethylacetoacetate did not lead to α,β-unsaturated isoxazole, so aliphatic aldehyde does not react in these conditions.

Table 4. Screening of the reaction conditions of the model reaction of benzaldehyde, 2-naphthol and acetamide for the synthesis of 7a in the presence of Fe_3O_4@C-SO_3H MNPs[a]

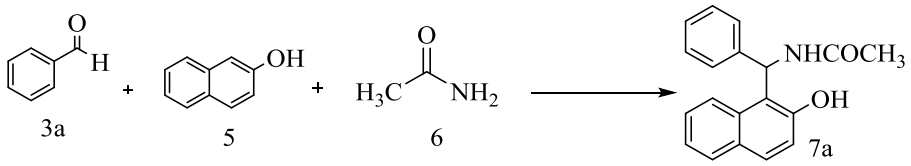

Entry	Catalyst (g)	mmol H^+	T (˚C)	Solvent (5 mL)	Time (min)	Yield (%)
1	0.03	0.039	70	Solvent-free	40	70
2	0.04	0.052	70	Solvent-free	40	95
3	0.05	0.065	70	Solvent-free	40	90
4	-	0	70	Solvent-free	120	10
5	0.04	0.052	Reflux	EtOH	120	25
6	0.04	0.052	Reflux	H_2O	120	10
7	0.04	0.052	Reflux	n-Hexane	120	0
8	0.04	0.052	25	Solvent-free	60	5
9	0.04	0.052	Reflux	CH_3CN	120	10

[a] Reaction conditions: benzaldehyde (1 mmol), 2-naphthol (1 mmol), acetamide (1 mmol) in the presence of Fe_3O_4@C-SO_3H MNPs under various conditions.

Table 5. Scope of aldehydes and amide studied for the synthesis of 1-amido alkyl-2-naphthols (**7a–l**) catalyzed by Fe_3O_4@C-SO_3H MNPs [a, b]

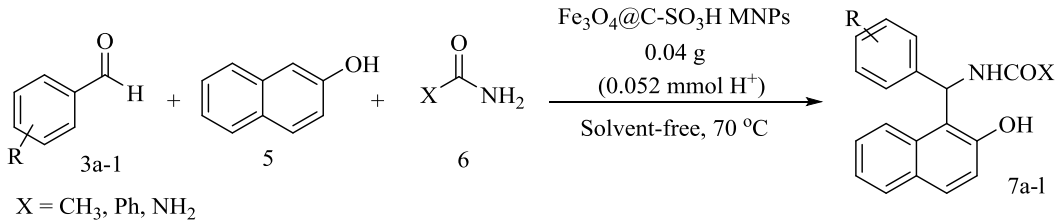

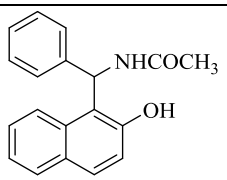	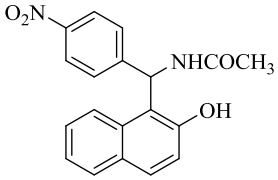	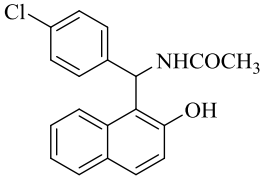	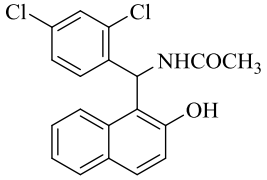
7a; 95% 40 min 228-230 ˚C	**7b**; 98% 20 min 239-241 ˚C	**7c**; 98% 25 min 236-238 ˚C	**7d**; 96% 30 min 230-232 ˚C
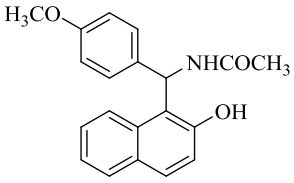	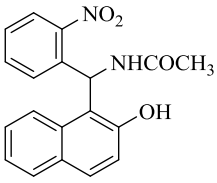	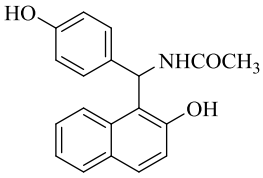	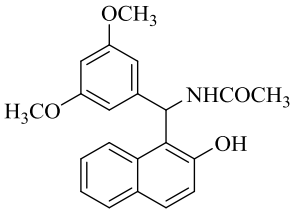
7e; 93% 28 min 184-186 ˚C	**7f**; 91% 25 min 179-181 ˚C	**7g**; 100% 30 min 218-220 ˚C	**7h**; 95% 25 min 253-255 ˚C
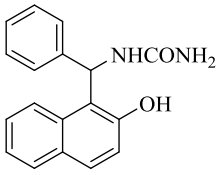		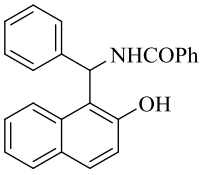	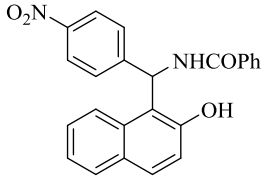
7i; 94% 30 min 178-180 ˚C	**7j**; 93% 20 min 190-192 ˚C	**7k**; 90% 15 min 230-232 ˚C	**7l**; 90% 20 min 239-241 ˚C

[a] Reaction conditions: aromatic aldehyde (1 mmol), 2-naphthol (1 mmol), acetamide (1 mmol) in the presence of Fe_3O4@C-SO_3H MNPs (0.04 g) at 70 ˚C under Solvent-free conditions. [b]Melting points are listed in Refs: [30-35].

*3.2.3.Synthesis of pyrano[2,3-c]pyrazole derivatives **(10a–l)***

The catalytic performance of Fe_3O_4@C-SO_3H MNPs has also been investigated in the synthesis of pyrano[2,3-c] pyrazoles. As an initial test, we run a model reaction by stirring an equimolecular amounts of benzaldehyde with hydrazine hydrate, ethyl acetoacetate (EAA), and malononitrile in the presence of Fe_3O_4@C-SO_3H MNPs (0.03 g) in water (5 mL) at 25 °C that result in the formation of the desired compound 1a with 90% yield (**Table 6**). To seek an optimal solvent and optimal amounts of catalyst, the model reaction was explored using different solvents such as water, ethanol, ethyl Acetate, *n*-Hexane and solvent-free conditions at room temperature. Also, to optimize the Fe_3O_4@C-SO_3H MNPs loading, the model reaction was performed with different amounts of catalysts at ambient temperature. And the important thing is that without the use of catalysts, the reaction did not proceed. The results are summarized in **Table 7.**

The scope of the response was then expanded to various benzaldehydes, including a range of electron-releasing or electron-withdrawing groups (**Table 7**). As shown in **Table 7** both, electron-donating and electron-withdrawing groups lead to the corresponding products in excellent yields.

Table 6. Screening of the reaction conditions of the model reaction of benzaldehyde, hydrazine hydrate, ethyl acetoacetate (EAA), and malononitrile for the synthesis of 10a in the presence of Fe_3O_4@C-SO_3H MNPs[a]

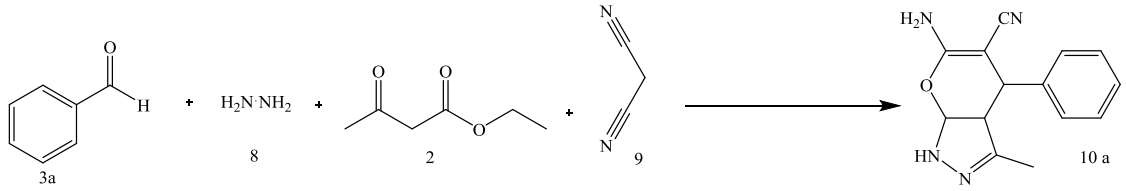

Entry	Catalyst(g)	mmol H^+	T (˚C)	Solvent(5 mL)	Time (min)	Yield (%)
1	0.02	0.026	25	H_2O	30	70
2	0.03	0.039	25	H_2O	30	90
3	0.04	0.052	25	H_2O	30	90
4	-	0	25	H_2O	120	10
5	0.03	0.039	25	EtOH	60	65
6	0.03	0.039	Reflux	H_2O	30	90
7	0.03	0.039	25	n-Hexane	120	0
8	0.03	0.039	25	Solvent-free	60	15
9	0.03	0.039	25	EtOAc	120	10

[a] The reaction conditions: benzaldehyde (1.0 mmol), hydrazine hydrate (1.0 mmol), ethyl acetoacetate (1.0 mmol), and malononitrile (1.0 mmol) in the presence of Fe_3O_4@C-SO_3H MNPs under variuos conditions.

Table 7. Scope of aldehydes and hydrazine hydrate studied for the synthesis of pyrano[2,3-c]pyrazole derivatives **(10 a–l)** catalyzed by Fe_3O_4@C-SO_3H MNPs[a]

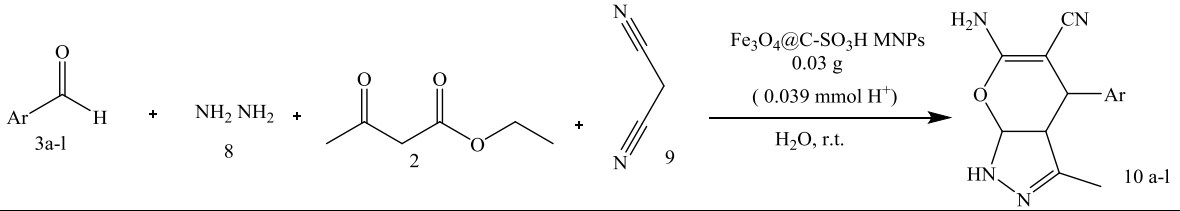

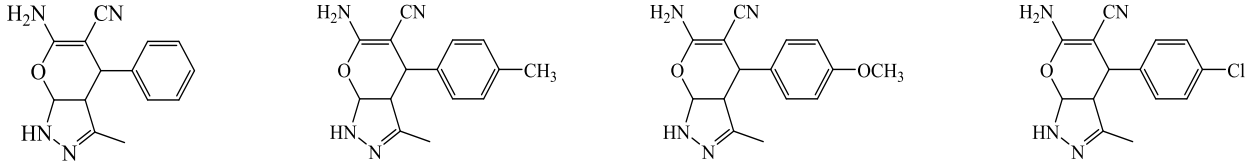

10a; 90%
30 min
242-244 ˚C

10b; 90%
20 min
193-195 ˚C

10c; 95%
17 min
208-210 ˚C

10d; 90%
15 min
230-232 ˚C

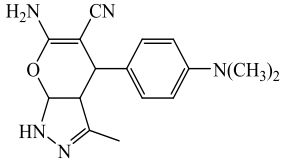

10e; 97%
35 min
215-217 ˚C

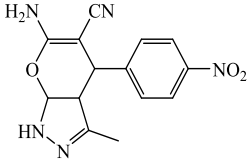

10f; 95%
20 min
248-250 ˚C

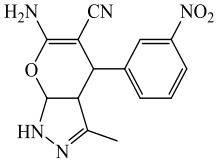

10g; 94%
20 min
235-237 ˚C

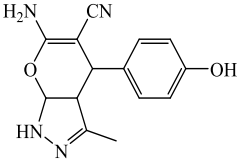

10h; 91%
30 min
225-227 ˚C

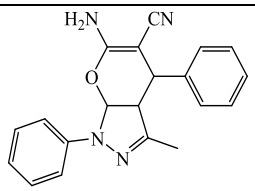	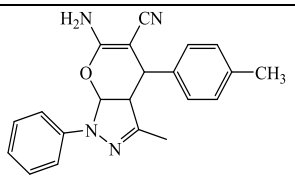	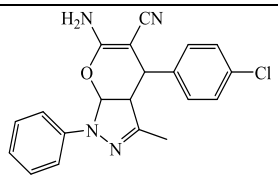	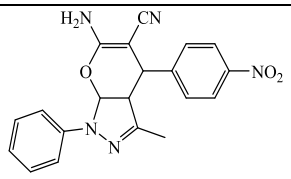
10i; 93%	**10j**; 90%	**10k**; 91%	**10l**; 92%
40 min	45 min	35 min	30 min
169-171 ˚C	180-182 ˚C	173-175 ˚C	189-191 ˚C

[a]The reaction conditions: aldehyde (1.0 mmol), hydrazine hydrate (1.0 mmol), ethyl acetoacetate (1.0 mmol), and malononitrile (1.0 mmol) in the presence of Fe_3O_4@C-SO_3H MNPs under variuos conditions. [b] Melting points are listed in Refs: [45-49].

*3.2.4.Synthesis of 2,3-dihydro quinazolin-4(1H)-ones **(12a–l)***

The activity of the catalyst was then investigated by employing it in the synthesis of 2,3-dihydroquinazolin-4(1*H*)-one derivative using the reaction of various benzaldehyde and 2-amino benzamide in aqueous media at room temperature. To find the best conditions, the reaction between benzaldehyde, and 2-amino benzamide was chosen as a model reaction. The influences of various parameters such as reaction temperature, solvent, amount of catalyst were examined to obtain the best possible combination (**Table 8**). Initially, coditions with a series of solvents, including H_2O, n-Hexane, EtOH, EtOAc, and in the absence of solvent (solvent-free condition) were studied in the presence of 0.03 g of prepared catalyst. Next, the catalyst loading under the aqueous condition and the effect of temperature on the model reaction were examined. The results were summarized in **Table 8**. The best results were gained with 0.03 g catalyst in aqueous media at room temperature. The increased temperature and the addition of more catalyst amounts did not lead to better results (reaction time and yield). And the important thing is that without the use of catalysts, the reaction did not proceed.

The scope of the reaction was then expanded to various benzaldehydes, including a range of electron-releasing or electron-withdrawing elements (Table 9). As shown in **Table 9** both electron-donating and electron withdrawing groups lead to the corresponding products in excellent yields.

Table 8. Screening of the reaction conditions of the model reaction of benzaldehyde and 2-amino benzamide for the synthesis of **12a** in the presence of Fe_3O_4@C-SO_3H MNPs.[a]

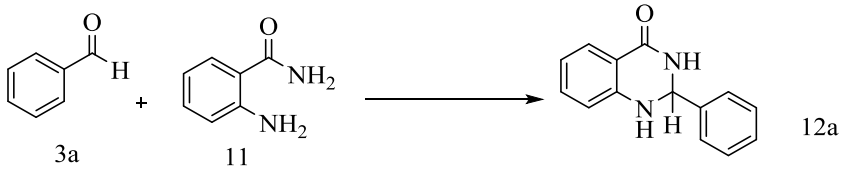

3a 11 12a

Entry	Catalyst (g)	mmol H^+	T (˚C)	Solvent (5 mL)	Time (min)	Yield (%)
1	0.02	0.026	25	H_2O	20	85
2	0.03	0.039	25	H_2O	20	100
3	0.04	0.052	25	H_2O	20	94
4	-	0	25	H_2O	60	5
5	0.03	0.039	25	EtOH	80	120
6	0.03	0.039	Reflux	H_2O	20	80
7	0.03	0.039	25	n-Hexane	120	0
8	0.03	0.039	25	Solvent-free	60	25
9	0.03	0.039	25	EtOAc	120	40

[a] The reaction conditions: benzaldehyde (1.0 mmol) and 2-amino benzamide (1.0 mmol) in the presence of Fe_3O_4@C-SO_3H MNPs at various conditions.[a]

Table 9. Scope of aldehydes studied for the synthesis of 2,3-dihydro quinazolin-4(1*H*)-ones (12a–l) catalyzed by Fe_3O_4@C-SO_3H MNPs [a, b]

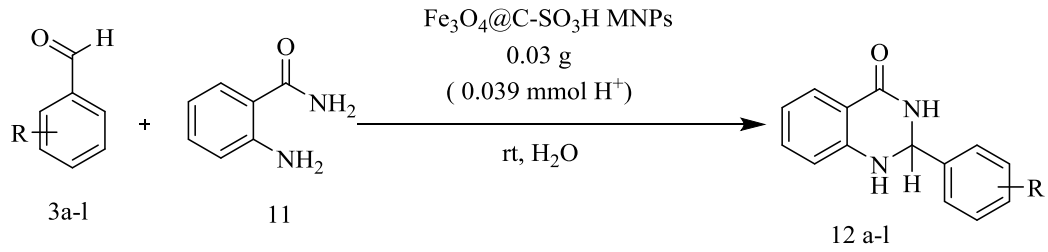

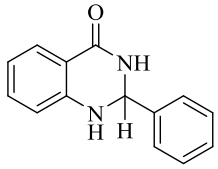	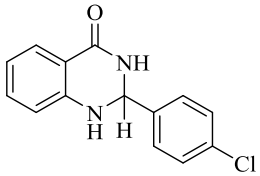	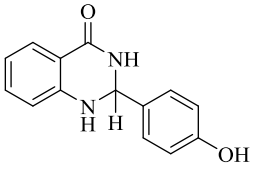	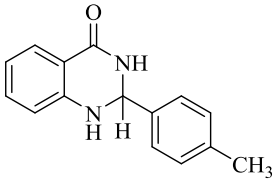
12a; 100% 20 min 225-227 ˚C	12b; 95% 8 min 200-202 ˚C	12c; 94% 10 min 213-215 ˚C	12d; 95% 20 min 229-231 ˚C
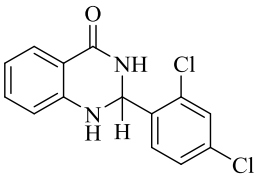	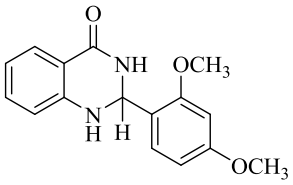	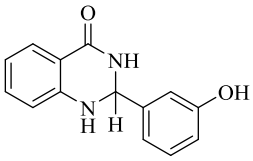	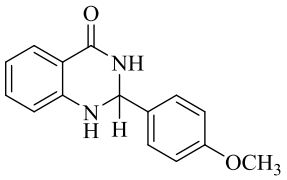
12e; 98% 15 min 182-184 ˚C	12f; 92% 10 min 179-181 ˚C	12g; 91% 25 min 220-222 ˚C	12h; 93% 17 min 185-187 ˚C
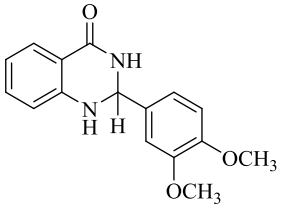	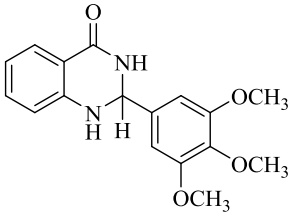	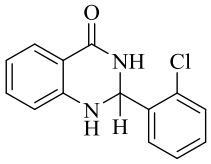	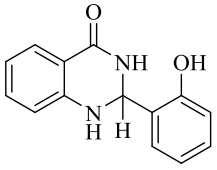
12i; 92% 10 min 174-176 ˚C	12j; 90% 10 min 188-200 ˚C	12k; 93% 15 min 209-211 ˚C	12l; 95% 25 min 200-202 ˚C

[a] The reaction conditions: benzaldehyde (1.0 mmol) and 2-amino benzamide (1.0 mmol) in the presence of Fe_3O_4@C-SO_3H MNPs (0.03 g) and H2O (5.0 mL) at rt.[b] Melting points are listed in Refs: [64-67].

3.2.5.Reusability of catalyst

The recyclability of the Fe_3O_4@C-SO_3H MNPs was investigated in the model reaction for the synthesis of 2-phenyl-2,3-dihydro quinazolin-4(1H)-one under optimized conditions (**Table 10**). After the reaction, the catalyst was separated by an external magnet. The recovered catalyst was reused six times without any significant decrease in the yield of the corresponding heterocyclic compound.

After the second and third runs, the acid densities of Fe_3O_4@C-SO_3H catalysts were measured by NaOH titration. It is clear from **Table 11** that the activity test results in the slight losses of acid densities from the 1.30 to 1.20 mmol/g, after the first and second runs, respectively, possibly due to the leaching of surface SO_3H groups.

On the other hand, the FT-IR spectrum of recycled catalyst and unused catalyst was shown in **Fig. 2**. The recycled catalyst after the second run was similar to the unused catalyst.

The performance and efficiency of the synthesized acidic Fe_3O_4@C-SO_3H nanocatalyst were compared with those of other synthesized catalysts in **Table 12**.

Table 10. Reusability of catalyst in the synthesis of 2-phenyl-2,3-dihydroquinazolin-4(1*H*)-one

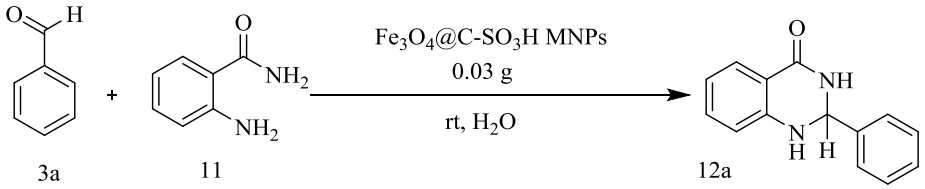

3a 11 12a

Run	Fresh	Run 1	Run2	Run3	Run 4	Run 5	Run6
Time (min)	20	20	20	20	20	20	20
Yield %	100	98	98	96	95	95	90

Table 11. Acidity density of Fe_3O_4@C-SO_3H catalyst during the catalytic runs

Catalyst	Acid density/(mmol g^{-1})
Fresh	1.30
After the first run	1.20
After the second run	1.20

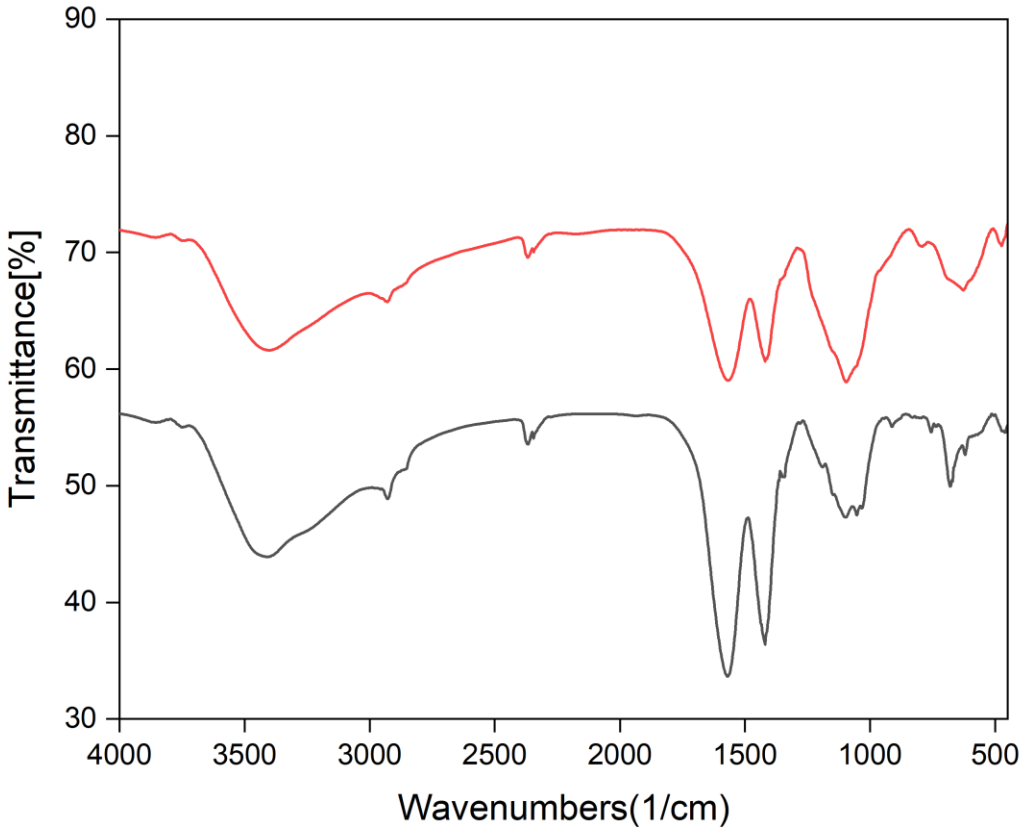

Fig. 2. FT-IR spectrum of unsed catalyt (Black) and the recycled catalyst (red)

Table 12. Comparison of acidity of the Fe_3O_4@C–SO_3H nanocatalyst with several known catalysts

Entry	Catalyst	Acidity	Reference
1	Pis-SO_3H	7.75	[77]
2	Pine-SO_3H	8.1	[78]
3	GPW-SO_3H	6.5	[79]
4	Str-SO_3H	0.19	[80]
5	Fe_3O_4@SiO_2@RF–SO_3H	1.30	]85[
6	Fe_3O_4@C-SO_3H	1.30	[86]
7	Fe_3O4@C-SO_3H	1.30	This work

3.2.6.Anti-microbial activity

The synthesized compounds were subject to antimicrobial screening by disk diffusion assay for the zone of inhibition. The Anti-bacterial activity of some derivatives was tested against gram-positive and gram-negative bacteria (**Fig. 3**).

The results were described in **Table 13**. According to the data (inhibition zone %) in **Table 13**, these compounds showed good activity against E. coli and Staphylococcus aureus.

4. Conclusions

In summary, the synthesis of Fe_3O_4@C-SO_3H as a magnetic carbon-based solid acid nanocatalyst from green pistachio peel (a biomass waste) is reported. The Fe_3O_4@C-SO_3H MNPs have been synthesized through hydrothermal carbonization and sulfonation. This new heterogeneous nanocatalyst has been efficiently used for the synthesis of isoxazole-5(4*H*)-one, 1-amido alkyl-2-naphthol, pyrano[2,3-c]pyrazole and 2,3-dihydro quinazolin-4(1*H*)-one derivative. All the reactions worked efficiently in high yields. More importantly, this nanocatalyst was recycled and used repetitively six times without a distinct loss of catalytic efficiency. The use of these magnetically recoverable catalysts has several advantages such as clean reaction profiles, lack of side reactions, green synthesis, simple experimental procedure, excellent catalytic performance, easy preparation from waste biomass, and simple magnetic attraction recovery process of the catalyst make it a suitable magnetically recyclable catalyst for several acid-catalyzed reactions.

Fig. 3. The biological activity of 2-phenyl-2,3-dihydro quinazolin-4(1*H*)-one

Table 13. The biological activity of some of the synthesized compounds 1-12

Entry	Product	Zone of Inhibition (mm)	
		Gram positive	Gram negative
		Staphylococcus aureus	Escherichia Coli
1	4a	14	12
2	4b	12	14
3	4c	10	10
4	7a	13	15
5	7b	10	11
6	7c	16	13
7	10a	15	15
8	10b	9	12
9	10c	8	9
10	12a	9	10
11	12b	10	10
12	12c	8	9
13	St	30	20

St., standard (Azithromycin).

Acknowledgements

The authors are thankful to Damghan University Research Council.

References

[1]. N. Poomathi, S. Mayakrishnan, D. Muralidharan, R. Srinivasan, P.T. Perumal, Green Chem. 17, (2015) 3362-3372.

[2]. E. Ruijter, R. Scheffelaar, R.V.A. Orru, Angew. Chem. Int. Ed. 50, (2011) 6234-6246.

[3]. H. Kiyani, F. Ghorbani, J. Saudi Chem. Soc. 18, (2014) 689.-701

[4]. S. P. N. Sudhan, R. Nasir Ahmed, H. Kiyani, S. Sheik Mansoor, J. Saudi Chem. Soc. 22, (2018) 269-278.

[5]. H. Kiyani, Curr. Org. Synth. 15, (2018) 1043-1052.

[6]. Y. Gu, W. Huang, S. Chen, X. Wang, Org. Lett. 14, (2018) 4285-4293.

[7]. J. Xu, W. Huang, R. Bai, Y. Queneau, F. Jérôme, Y. Gu, Green Chem. 21, (2019) 2061-2069.

[8]. N. Agrawal, P. Mishra, Med. Chem. Res. 27, (2018) 1309-1321.

[9]. S. S. Wazalwar, A. R. Banpurkar, F. Perdih, J. Mol. Struct. 1150, (2017) 258.-267

[10]. A.R. Banpurkar, S.S. Wazalwar, F. Perdih, Bull. Chem. Soc. Ethiop. 32, (2018) 249.-257

[11]. S. J. Kim, J. Yang, S. Lee, C. Park, D. Kang, J. Akter, S. Ullah, Y. J. Kim, P. Chun, H. R. Moon, Bioorg. Med. Chem. 26, (2018) 3882-3889.

[12]. M. Lavanya, M. Jagadeesh, J. Hari Babu, R. Karvembu, H.K. Rashmi, P. Uma Maheswari Devi, A.V. Reddy, Inorganica Chimica Acta 469, (2018) 76-86.

[13]. B. Kafle, H. Cho, Bull. Korean Chem. Soc. 33, (2012) 275-277.

[14]. Y. Kazui, S. Fujii, A. Yamada, M. Ishigami-Yuasa, H. Kagechik, A. Tanatani, Bioorg. Med. Chem. 26, (2018) 5118.-5121

[15]. M. Tang, S. I. Odejinmi, Y. M. Allette, H. Vankayalapati, K. Lai, Bioorg. Med. Chem. 19, (2011) 5886.-5895

[16]. S. Breuer, M. W. Chang, J. Yuan, B. E. Torbett, J. Med. Chem. 55, (2012) 4968-4977.

[17]. Ş. G. Kömürcü, S. Rollas, N. Yilmaz, A. Çevikbaş, Drug Metabol. Drug Interact. 12, (1995) 161-166.

[18]. W. Hallenbach, O. Guth, T. Seitz, H. J. Wrolowsky, P. Desbordes, U. Wachendorff-Neumann, P. Dahmen, E. Voerste, P. Lösel, O. Malssm, R. Rama, H. Hadano, US Patent, Pub. No.: US 2012/0065063A1 (2012).

[19]. A. H. Reshak, S. Azam, Mater. Sci. Semicond. Process. 30, (2015) 197-207.

[20]. A. F. da Silva, A. A. G. Fernandes, S. Thurow, M. L. Stivanin, I. D. Jurberg, Synthesis 50, (2018) 2473-2489.

[21]. T. Ghosh, A. Gopal, A. Saeki, S. Sekic, V. C. Nair, Phys. Chem. Chem. Phys. 17, (2015) 10630-10639.

[22]. H. Kiyani, F. Ghorbani, J. Saudi Chem. Soc. 21, (2017) S112.-S119

[23]. H. Kiyani, F. Ghorbani, Res. Chem. Intermed. 41, (2015) 7847-7882.

[24]. H. Kiyani, M. Jabbari, A. Mosallanezhad, Jordan J. Chem. 9, (2014) 279-284.

[25]. F. Ghorbani, H. Kiyani, S. A. Pourmousavi, Res. Chem. Intermed. 46, (2020) 943–959.

[26]. I. Mohanram, Meshram, J. Med. Chem. Res. 23, (2014) 939.

[27]. H. Darbandi, H. Kiyani, Curr. Organocatal. 7, (2020) 34-48.

[28]. Y. Kusakabe, J. Nagatsu, M. Shibuya, O. Kawaguchi, C. Hirose, S. Shirato, J. Antibiot. 25, (1972) 44.-47

[29]. J. L. Peglion, J. Vian, B. Gourment, N. Despaux, V. Audinot, M. Millan, Bioorg. Med. Chem. Lett. 7, (1997) 881-886.

[30]. G. Y. Lesher, A. R. Surrey, J. Am. Chem. Soc. 77, (1955) 636-647.

[31]. M. Karabacak, M. Kurt, J. Mol. Struct. 919, (2009) 215-222.

[32]. S. A. Pourmousavi, P. Moghimi, F. Ghorbani, M. Zamani, J. Mol. Struct. 1144, (2017) 87-102.

[33]. A. V. Shelke, B. Y. Bhong, N. N. Karade, Synthesis 46, (2014) 752-789.

[34]. G. Y. Lesher, A. R. Surrey, J. Am. Chem. Soc. 77, (1955) 636-654.

[35]. Y. Takeda, K. Yano, T. Kuroki, J. Med. Chem. 40, (1997) 105-111.

[36]. H. R. Shaterian, F. Rigi, Res. Chem. Intermed. 40, (2014) 2983-2999.

[37]. Z. Nasresfahani, M. Z. Kassaee, E. Eidi, New J. Chem. 40, (2016) 4720-4789.

[38]. M. Wang, Y. Liang, Monatsh. Chem. 142, (2011) 153-157.

[39]. A. S. Amarasekara, J. Nguyen, A. Razzaq, J. Polym. Res. 24, (2017) 52-79.

[40]. W. Chen, X. W. Peng, L. X. Zhong, Y. Li, R. C. Sun, Acs Sustain. Chem. Eng. 3, (2015) 1366-1373.

[41]. F. Ghorbani, H. Kiyani, S. A. Pourmousavi, Res. Chem. Intermed. 42, (2020) 2075-2084.

[42]. P. T. Mistry, N. R. Kamdar, D. D. Haveliwala, S. K. J. Patel, Heterocyclic Chem. 49, (2012) 349-357.

[43]. V. K. Ahluwalia, A. Dahiya, Garg, V. Indian J. Chem. 36B, (1997) 88-90.

[44]. J. L. Wang, D. Liu, Z. J. Zheng, S. Shan, X. Han, S. M. Srinivasula, C. M. Croce, E. S. Alnemri, Z. Huang, Proc. Natl. Acad. Sci. U.S.A. 97, (2009) 7124-7129.

[45]. M. E. A. Zaki, E. M. Morsy, F. M. Abdel-Motti, F. M. E. Abdel-Megeid, Heterocycl. Commun. 10, (2004) 97-102.

[46]. N. Foloppe, L. M. Fisher, R. Howes, A. Potter, A. G. S. Robertson, A. E. Surgenor, Bioorg. Med. Chem. 14, (2006) 4792-4802.

[47]. F. M. Abdelrazek, P. Metz1, O. Kataeva1, A. Jäger, S. F. El-Mahrouky, Arch. Pharm. Chem. Life Sci. 340, (2007) 543-548.

[48]. M. M. M. Ramiz, I. S. Abdel Hafiz, M. A. M. Abdel Reheim, H. M. J. Gaber, Chin. Chem. Soc. 59, (2012) 72-80.

[49]. H. Wamhoff, E. Kroth, K. Strauch, Synthesis. 11, (1993) 1129-1132.

[50]. D. Armetso, W. M. Horspool, N. Martin, A. Ramos, C. Seaone, J. Org. Chem. 54, (1989) 3069-3072.

[51]. Y. A. Sharanin, L. N. Shcherbina, L. G. Sharanina, V. V. Zh. Puzanova, Org. Khim. 19, (1983) 164173.

[52]. T. S. Jin, R. Q. Zhao, T. S. Li, Arkivoc xi. (2006) 176-182.

[53]. S. Wang, A. Q. Cheng, Z. L. Zhang, J. S. Li, Synth. Commun. 35, (2005) 137-143.

[54]. N. R. Mohamed, N. Y. Khaireldin, A. F. Fahmyb, A. A. El-Sayeda, Der Pharma Chem. 2, (2010) 400-417.

[55]. H. V. Chavan, S. B. Babar, R. U. Hoval, B. P. Bandgar, Bull. Korean Chem. Soc. 32, (2011) 3963-3966.

[56]. S. B. Mhaske, N. P. Argade, Tetrahedron, 62, (2006) 9787-9826.

[57]. Y. Takaya, H. Tasaka, T. Chiba, K. Uwai, M.-a. Tanitsu, H.-S. Kim, Y. Wataya, M. Miura, M. Takeshita, Y. Oshima, Journal of medicinal chemistry, 42, (1999) 3163-3166.

[58]. Y. Xia, Z. Y. Yang, M.-J. Hour, S. C. Kuo, P. Xia, K. F. Bastow, Y. Nakanishi, P. Nampoothiri, T. Hackl, E. Hamel Bioorganic & medicinal chemistry letters, 11, (2001) 1193-1196.

[59]. R. J. Alaimo, H. E. Russell, Journal of medicinal chemistry, 15, (1972) 335-336.

[60]. M. J. Hour, L. J. Huang, S. C. Kuo, Y. Xia, K. Bastow, Y. Nakanishi, E. Hamel, K. H. Lee, Journal of medicinal chemistry, 43, (2000) 4479-4487.

[61]. H. Li, R. Huang, D. Qiu, Z. Yang, X. Liu, J. Ma, Z. Ma, Progress in Natural Science. 8, (1998) 359-365.

[62]. E. Honkanen, A. Pippuri, P. Kairisalo, P. Nore, H. Karppanen, I. Paakkari, Journal of medicinal chemistry. 26, (1983) 1433-1438.

[63]. A. Baba, N. Kawamura, H. Makino, Y. Ohta, S. Taketomi, T. Sohda, Journal of medicinal chemistry. 39, (1996) 5176-5182.

[64]. M. S. Malamas, J. Millen, Journal of medicinal chemistry. 34, (1991) 1492-1503.

[65]. N. P. Abida, M. Arpanarana, International Journal of Pharmaceutical & Biological Archive. 2, (2011) 1651-1657.

[66]. P. Nandy, M. Vishalakshi, A. Bhat, Indian Journal of heterocyclic chemistry. 15 (2006) 293-294.

[67]. S. Sasmal, G. Balaji, H.R.K. Reddy, D. Balasubrahmanyam, G. Srinivas, S. Kyasa, P.K. Sasmal, I. Khanna, R. Talwar, J. Suresh, Bioorganic & medicinal chemistry letters. 22, (2012) 3157-3162.

[68]. Y. Kurogi, Y. Inoue, K. Tsutsumi, S. Nakamura, K. Nagao, H. Yoshitsugu, Y. Tsuda, Journal of medicinal chemistry. 39, (1996) 1433-1437.

[69]. X. S. Wang, J. Sheng, L. Lu, K. Yang, Y.-L. Li, ACS combinatorial science. 13, (2011) 196-199.

[70]. M. Sharma, S. Pandey, K. Chauhan, D. Sharma, B. Kumar, P.M. Chauhan, The Journal of organic chemistry. 77, (2012) 929-937.

[71]. V. B. Labade, P. V. Shinde, M. S. Shingare, Tetrahedron Letters. 54, (2013) 5778-5780.

[72]. M. R. M. Shafiee, Journal of Saudi Chemical Society. 18, (2014) 115-119.

[73]. A. Shaabani, A. Maleki, H. Mofakham, Synthetic Communications. 38, (2008) 3751-3759.

[74]. S. Rasheed, D. N. Rao, A. S. Reddy, R. Shankar, P. Das, Rsc Adv. 5, (2015) 10567-10574.

[75]. V. K. Rajput, B. Mukhopadhyay, Tetrahedron Lett. 47, (2006) 5939-5941.

[76]. J. Zhang, B. Zhang, J. Zhou, J. Li, C. Shi, T. Huang, Z. Wang, J. Tang, J. Carbohydr. Chem. 30, (2011) 657–662.

[77]. J. Zhang, B. Zhang, J. Zhou, H. Chen, J. Li, G. Yang, Z. Wang, J. Tang, J. Carbohydr. Chem. 32, (2013) 380-391.

[78]. J. F. Zhou, X. Chen, Q. B. Wang, B. Zhang, L. Y. Zhang, A. Yusulf, Z. F. Wang, J. B. Zhanga, J. Tang, Chin. Chem. Lett. 21, (2010) 922-936.

[79]. O. Rosati, F. Messin, A. Pelosi, M. Curini, V. Petrucci, J. Gertsch, A. Chicca, Eur. J. Med. Chem. 85, (2014) 77-85.

[80]. B. Maleki, E. Sheikh, E. Rezaei Seresht, H. Eshghi, S. S. Ashrafi, A. Khojastehnezhad, H. Veisi, Org. Prep. Proced. Int. 48, (2016) 37-44

[81]. S. Roy, K. K. Senapati, P. Phukan, Res. Chem. Intermed. 41, (2015) 5753-5767.

[82]. M. Samadizadeh, S. Nouri, F. Kiani Moghadam, Res. Chem. Intermed. 42, (2016) 6089-6103.

[83]. M. M. Dutta, K. K. Rajbongshi, P. Phukan, Synth. Commun. 47, (2017) 2330-2341.

[84]. M. S. T. Rocha, J. Rafique, S. Saba, J. B. Azeredo, D. Back, M. Godoi, A. L. Braga, Synth. Commun. 47, (2017) 29-298.

[85]. M. Mamaghani, F. Shirini, M. Sheykhan, M. Mohsenimehr, RSC Adv. 5, (2015) 44524-44529.

[86]. F. Ghorbani, H. Kiyani, S. A. Pourmousavi, Current Organocatalysis. 7, (2020) 55-8.

[87]. X. Wang, R. Liu, M. M. Waje, Z. Chen, Y. Yan, K. N. Bozhilov, Chem. Mater. 19 (2007) 2395–2397.

[88]. M. Zhu, G. Diao, Magnetically. 115 (2011) 24743–24749.

[89]. T. Karimpour, E. Safaei, B. Karimi, RSC Adv. 9, (2019) 14343-14351.

[90]. M. Gupta, M. Gupta, Rajnikant, V. K. Gupta, New J. Chem. 39, (2015) 2395-3578.

[91]. S. M. Yuan, J. X. Li, L. T. Yang, L. W. Su, L. Liu, Z. Zhou, Mater. Interfaces. 3, (2011) 705–709

[92]. F. Ghorbani, S. A. Pourmousavi, H. Kiyani, Lett. Org. Chem. 18(1), (2021) 66-81.

[93]. F. Ghorbani, S. A. Pourmousavi, H. Kiyani, Curr. Org. Synth. 17(6), (2020) 440-456.

[94]. F. Ghorbani, S. A. Pourmousavi, H. Kiyani, Current Organocatalysis. 7(1), (2020) 55-80.

[95]. F. Z. Damghani, S. A. Pourmousavi, H. Kiyani, Curr. Org. Synth. 16(7), (2019) 1040-1054.

[96]. S. A. Pourmousavi, P. Moghimi, F. Ghorbani, M. Zamani, J. Mol. Struct. 1144, (2017) 87-102.

[97]. S. A. Pourmousavi, A. Kanaani, F. Ghorbani, F. Z. Damghani, D. Ajloo, M. Vakili, Res. Chem. Intermed. 42(2), (2016) 1237-1274.

[98]. Hoseinabadi, Z. Pourmousavi, S. A. Zamani, M. Res. Chem. Intermed. 42(6), (2016) 6105-6124.

[99]. Fahid, F. Pourmousavi, S. A. J. Sulphur Chem. 36(1), (2015) 16-29.